

# Topographic effects influencing large scale slope failure during the 21<sup>st</sup> of September Chichi earthquake, Taiwan, 1999.

Murphy, W.<sup>1</sup>, Petley, D. N.<sup>1</sup>, Risdon, G.<sup>1</sup> & Chen, M. C.<sup>2</sup>

<sup>1</sup> School of Earth, Environmental and Physical Sciences, Burnaby Building, Burnaby Road, Portsmouth. PO1 3QL. Contact e-mail: william.murphy@port.ac.uk

<sup>2</sup> Conservation and Research Division, Taroko National Park HQ, 291 Fu-Su Village, Hualien 97203, Taiwan ROC

## Abstract

The Central Cross Island Highway is a strategically important routeway through the Central Mountains of Taiwan. Strong shaking generated by the Chi Chi earthquake of 21st of September 1999 resulted in extensive slope failure that destroyed a section of the road to the west of the Techí Dam.

Detailed Investigation of the rock masses showed that these were dominantly mudstones, siltstones and shales which have been tilted to show a steep easterly dip. The rock masses can be rated as *good* or *poor* rock depending on the individual units. Landslide occurrence was correlated with the incidence of mudstone units in the stratigraphy. Analysis of the slope stability using a basic infinite slope model and rock mass cohesion and friction angles indicates a factor of safety, *F*, that would indicate long term stability. On this basis on these static factors of safety (*F*) it is possible to estimate the critical acceleration required to induce movement of the slope. It was found that the ground motions required to cause movement of the slope were 2-3 times higher than which is indicated by strong motion instruments in the area. It is believed that the combination of a weak, fractured rock mass along with the steep slopes gave rise to topographic amplification which resulted in anomalously high shaking leading to slope failure. It is noteworthy however, that the values of spectral acceleration (*S<sub>a</sub>*) calculated from selected strong motion data shows values in a similar range to those accelerations required to cause slope movement. It seems likely that the use of a peak horizontal ground acceleration is less well suited to a slope stability analysis during earthquakes than *S<sub>a</sub>* at a frequency range appropriate to the rock mass under investigation.

*landslides, topographic amplification, spectral acceleration.*

## 1. INTRODUCTION

### 1.1 Geographic Setting

Taiwan is an island approximately 8% of the size of California located off the southeast coast of China. The island has a sub-tropical environment that experiences intense seasonal rainfall during the typhoon season (July – October). Rainfall intensities may exceed 1500 mm in 24 hours during typhoons. Taiwan is affected by an average of 3.5 typhoons per year. This intense rainfall gives rise to severe landslide problems.

The problems associated with typhoons is exacerbated by the occurrence of steep slopes which are an effect of the rapid tectonic uplift experienced by the island. Rates of uplift in the Central Mountains have been estimated to be in the order of 10  $\text{mma}^{-1}$ . This rapid uplift is balanced by high denudation rates.

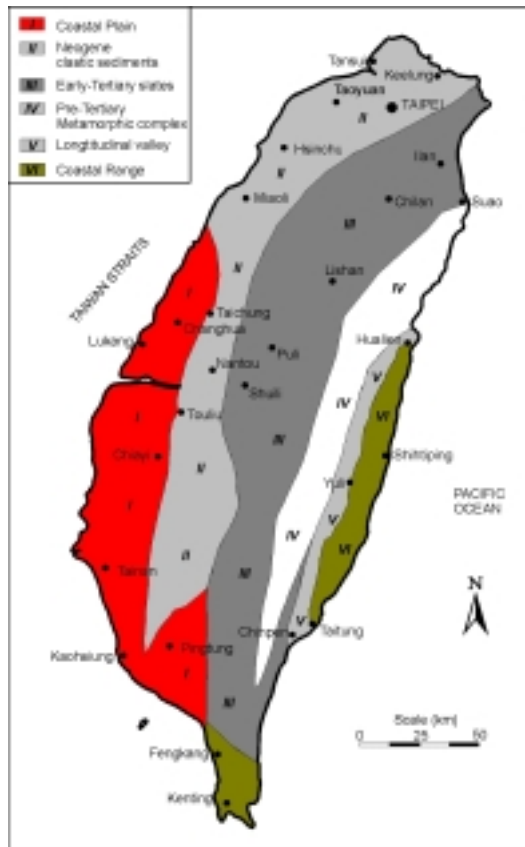


Figure 1. The general geology of Taiwan

## 1.2 Geology

The geology of Taiwan can be broadly divided into five lithostructural domains which generally get younger towards the west of the island. This situation is complicated by the presence of the Longitudinal Valley on the eastern side of the Island which is dominated by geologically young deposits. This zone also marks a major tectonic boundary.

The oldest units which are found in Taiwan are the marbles and gneisses of the pre-Tertiary metamorphic complex (figure 1) Only occasional rock slope failures were triggered in these rocks by the earthquake. Overlying these rocks are the early Tertiary slates which in turn are overlain by a group of Neogene clastic sedimentary rocks which are dominantly sandstones, siltstones and shales. These Neogene rocks have been deformed, although sedimentary structures can still be observed, as can occasional fossil fauna. The youngest rocks are generally found on the western coastal plain. These are Quaternary clastic sediments which showed liquefaction during the Chi Chi earthquake. The geology of the site under investigation is dominated by Neogene clastic

sedimentary rocks.

## 1.3 Regional Seismicity & Tectonics

The regional seismicity is dominated by the effects of the two major trench systems found near Taiwan. The north of the island is dominated by the northward subduction of the Philippine Sea plate beneath the Eurasian plate (The Ryukyu Arc), while to the south, the Eurasian plate is being subducted below the Philippine Sea plate at the Luzon Arc. The oblique convergence of the Philippine Sea Plate has led to zone of strike-slip deformation to the east of Taiwan and in the Longitudinal Valley. An examination of tectonic landforms from LANDSAT data shows that there is evidence for strike-slip tectonics east of the Longitudinal Valley, but little evidence for such features to the west. Indeed a reasoned interpretation of the landforms would suggest that active extension is occurring to the west of the longitudinal valley. However, focal plane solutions for large earthquakes in this region indicate a dominantly compressive environment. It is likely that rapid uplift rates in the mountains is leading to extensional landforms through footwall uplift, but that deeper compressional forces are driving the earthquake activity.

Rates of convergence between the Philippine Sea Plate and the Australasian plates are in of the order of  $70-75 \text{ mma}^{-1}$  in an orientation which is oblique to the coast of the island

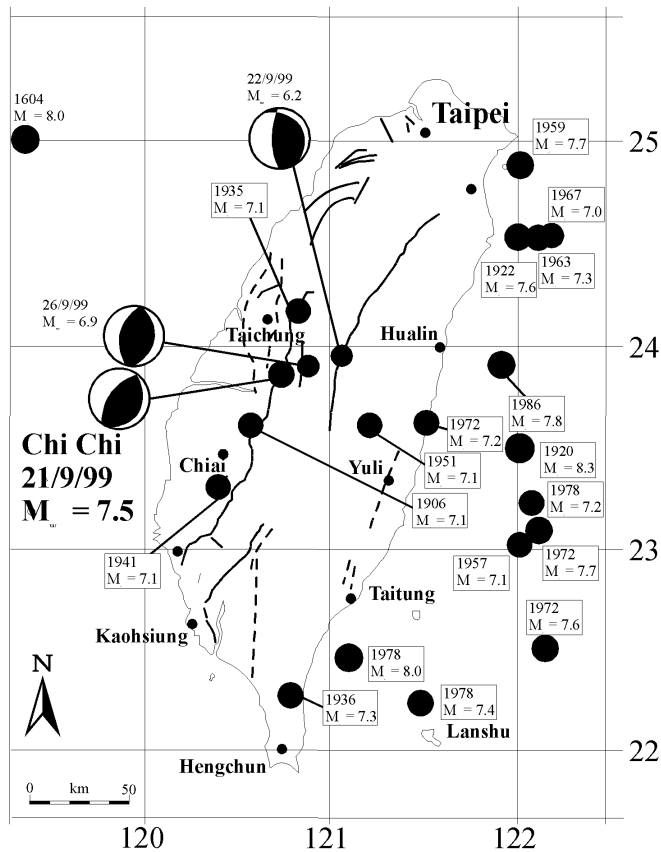


Figure 2. Earthquakes of  $M > 7.0$  in the Taiwan region since 1640 (USGS database).

Therefore, the majority of seismic energy release occurs to the east of the Taiwan landmass. Figure 2 shows the distribution of earthquakes of  $M > 7.0$  from the instrumental and historical records. The focal plane solution of the Chi Chi earthquake and associated large aftershocks can also be seen.

## 2. THE CHI CHI EARTHQUAKE

### 2.1 Faulting and seismic effects

The Chi Chi earthquake of 21st September 1999 was due to between 6 and 9 m of reverse slip on a 80 km segment of the Chelongpu Fault (Bilham & Yu, 2000). This structure forms one of the frontal thrusts at the base of the mountains. The focal plane solution indicated almost pure compression with a rake of  $30-38^\circ$ . This is consistent with field observations of rake from slickensides reported on the fault surface by Bilham and Yu (2000). The earthquake was unusually shallow focus (approximately 5 km).

The earthquake appears to have been a complex source event with two events being separated by an approximately 12 seconds. Maximum energy release occurred some 25 km north of the point of first rupture on what appears to be, on the basis of morphological data, a fault jog. The resulting acceleration field was recorded by a dense set of instrumentation. Peak horizontal ground accelerations were reported as 0.98g (E-W), 0.64 g (N-S) and 0.51 g (vertical) (Shin *et al*/2000). The highest ground motions were experienced to the east of the Chelongpu fault. The duration of shaking lasted approximately 20-30 seconds in the nearfield regions and was followed by a highly energetic aftershock sequence with three events of  $m_b > 6.0$  in the following 48 hours. Strong aftershocks from this earthquake are still being felt in western Taiwan.

The earthquake gave rise to extensive ground failure in western Taiwan. These can be split into two categories: liquefaction induced failures (which were largely limited to the youngest geological unit in the west, especially at Taichung) and earthquake-triggered landslides. It is the latter group of phenomena which is the subject of this paper.

### 3. LANDSLIDES TRIGGERED BY THE EARTHQUAKE

#### 3.1 General remarks

Landslides were triggered by this earthquake as far away as Taroko Gorge. While a total inventory of landslides triggered by the earthquake is still being compiled from aerial photography taken immediately after the event, it is possible to make some general observations.



Figure 3. Damage to highway 8 by a seismically-triggered landslide near Lishan

Firstly, the majority of landslides observed were rockfalls, rockslides and debris slides (Varnes, 1978) and all fall into the 'disrupted slide' category of Keefer (1984). Many failures occurred where slopes have been oversteepened due to river erosion or road construction (figure 3). Two notable exceptions to this observation were the landslides at Chefengershan near Puli and the reactivation of the Tsaoling landslide. These two catastrophic failures were approximately 30,000,000 m<sup>3</sup> and 120,000,000 m<sup>3</sup> respectively. The former of these two failures destroyed approximately 20 houses, killing 40 people.

A survey of landslides was carried out during a two week period of fieldwork after the earthquake. Landslides were divided into categories as described by Varnes (1978) for rapid classification. In addition to the normal landslide classification schemes an additional class of slope failure was introduced which represented small strain failures. These landslides show small displacements (normally less than 100 mm) that were insufficient for the residual strength to be reached. Therefore, these represent incipient slope failure which, in some cases, continued to move. One such example near Kuanyuan showed a displacement of 110 mm after the earthquake but was found to have a displacement of approximately 1.5 m at the head of the slide in July 2000. It is difficult to say how widespread such failures were due to the heavily wooded terrain, and the road survey must be viewed as a minimum.

Examination of figure 4 shows that there is an increasing density of landslides along the road which increases from east to west. It is interesting to note however, that this increase is not uniform and that the Central Cross Island Highway (I8) shows a higher density of slope failures than I14. There are two likely reasons for this. Firstly, the terrain is generally steeper and more mountainous in this region, secondly, this is in fact closer to the area of greatest energy release.

#### 3.2 Landslides on the Central Cross Island Highway (I8)

While numerous slope failures occurred on this section of road, it remained largely passable until west of the Techu Dam. At the entrance to the dam control buildings I8 divides in two, consisting of an upper (westbound) section and a lower (eastbound) carriageway. At this site, the road was badly damaged by 21 rockslide / debris slide landslides and a rock block slide. The road was severed by a single wedge failure which undermined the lower of the two carriageways.

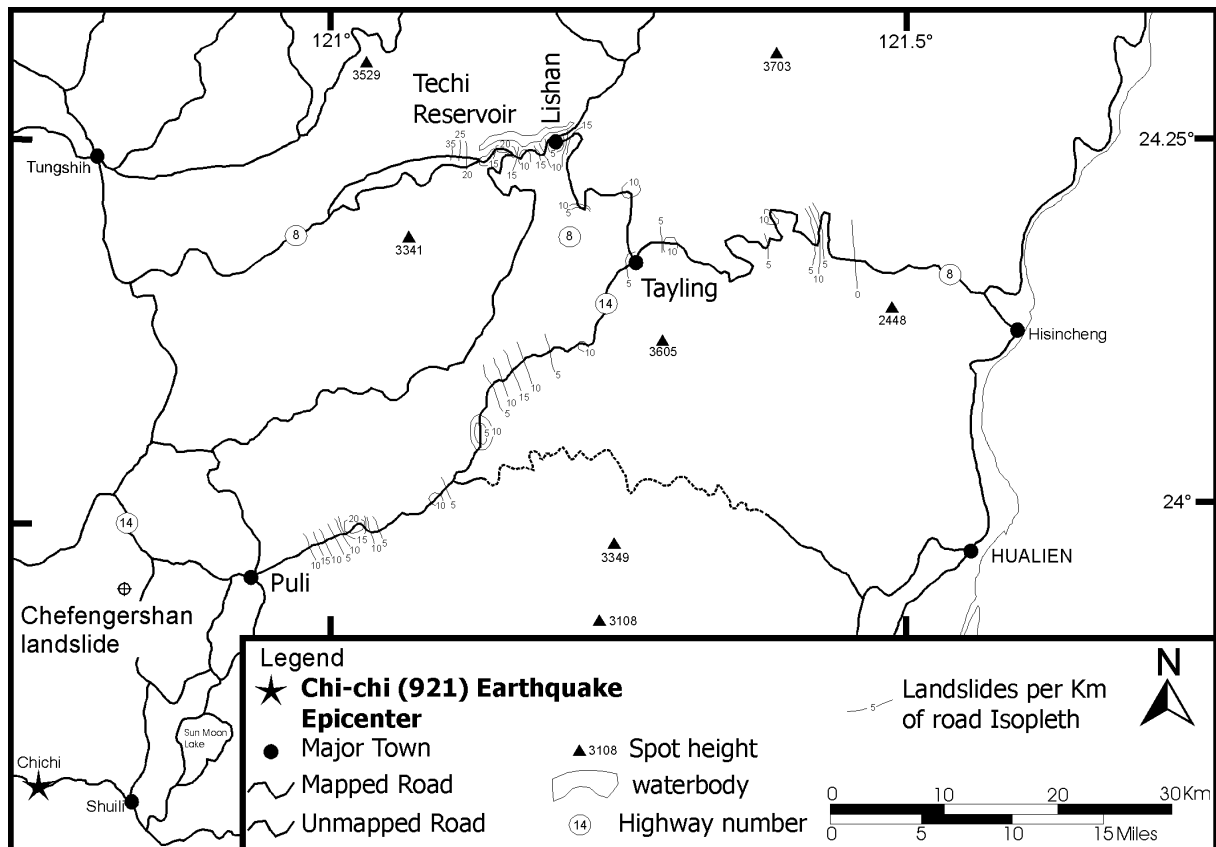


Figure 4. Map showing increasing density of landsliding triggered by the Chi Chi earthquake on highway 14 (south) and Highway 8 (north)

The local geology around the site was varied but not overly complex. The dam site itself is dominated by folded and faulted sandstones, siltstones and shales. There is a strong easterly dip to the bedding of about  $72^\circ$ . The bedding forms the dominant discontinuity, therefore the orientation of major fracture planes is not conducive to large scale slope failure. The rock mass is shown in figure 5.

Numerous faults strike through the area which can be identified both on aerial photographs and in the rock cuttings which forms the slopes. While many of these structures appear to be minor, a major fault occurs close to where the dam has been built. This juxtaposes two large lithological groups (Shieh, 1991). To the east of this fault, the stratigraphy is dominated by a larger proportion of mudstone units. Geomorphologically, this results in a wider valley. To the west of this fault, the stronger sandstone units dominate, and the river valley is considerably narrower and steeper. Therefore this part of the road is naturally more susceptible to landslides.

### 3.3 Seismically-triggered landslides near Tech

In order to investigate the reasons for the slope failures which were observed near Tech a detailed rock mass investigation was carried out, along with a geomorphological survey of the landslides along the road. Data were collected to allow the Rock Mass Rating (RMR) of Bieniawski (1989) and the Geological Strength Index (GSI) of Hoek (1994) to be calculated. Samples were also collected to allow characterization of both the rock material and the rock mass using the Hoek-Brown failure criterion.



Figure 5. The rock mass observed at the Techi landslides

On the basis of these data the stability of the slope was then calculated using a relatively simple factor of safety calculation. In this case, the infinite slope model (see Jibson & Keefer, 1993) was used and further calculations were calculated on the basis of a Newmark Sliding Block Model (Newmark, 1965). Of the 23 (figure 6 and 7) landslides which were identified by ground survey and aerial photography, 21 were analyzed using this method. The remaining two slides were strongly controlled by the presence of geological discontinuities that violate key assumptions in the use of RMR and GSI methods in this way.

Rock mass properties were carefully assessed for each geological unit exposed in the road cutting.

Each landslides was back analyzed using the parameters shown in Table 1. Two forms of analysis were carried out. The first involved analysis of the stability of the slope using mean values of RMR measured for different units over the breadth of the landslide, the second used the 'worst case' scenario in which it was assumed that the weaker mudrock units controlled failure. Shieh (1991) observed, on the basis of down hole piezometer observations, that the groundwater level was as much as 40 m below the ground surface, therefore pore water pressures were assumed to be zero.

It is notable that the factors of safety (the ratio of shear strength to shear stress) indicated by this analysis are greater than 1. In fact, these values are significantly greater than 1 which is a function of the model used. The higher this value, the greater the stability of the slope.

Geomorphic evidence which shows few landslides of this type in the area, although rock falls and rock topples are common, and it has been necessary to remediate against these hazards to ensure the safety of the road. Debris slides / debris flows type landslides are only common around gullies (one of which can be seen immediately to the east of the Techi Dam. The landslides triggered by the earthquake of the 21<sup>st</sup> of September do not have an origin in this geomorphological regime.



Figure 6. Overview of the landslides near the Techi Dam

|                   | 1     |       | 2     |       | 3     |       | 4     |       | 5     |        |
|-------------------|-------|-------|-------|-------|-------|-------|-------|-------|-------|--------|
|                   | mean  | min   | mean  | min   | mean  | min   | mean  | min   | mean  | min    |
| RMR               | 46.2  | 25    | 33    | 25    | 50    | 24    | 55    | 29    | 54    | 19     |
| c'                | 12    | 9     | 10    | 9     | 13    | 9     | 13    | 10    | 13    | 9      |
| $\phi$            | 49    | 31    | 37    | 31    | 52    | 31    | 56    | 35    | 55    | 27     |
| Z                 | 25    | 25    | 5     | 5     | 7.5   | 7.5   | 7.5   | 7.5   | 7.5   | 7.5    |
| $\alpha$          | 36    | 36    | 38    | 38    | 38    | 38    | 38    | 38    | 38    | 38     |
| F                 | 1.99  | 1.05  | 1.37  | 1.11  | 2.21  | 1.06  | 2.54  | 1.24  | 2.45  | 0.92   |
| A <sub>crit</sub> | 0.582 | 0.029 | 0.228 | 0.068 | 0.745 | 0.037 | 0.948 | 0.148 | 0.893 | -0.049 |

|                   | 6     |        | 7     |       | 10    |       | 11    |       | 12    |       |
|-------------------|-------|--------|-------|-------|-------|-------|-------|-------|-------|-------|
|                   | mean  | min    | mean  | min   | mean  | min   | mean  | min   | mean  | min   |
| RMR               | 47    | 19     | 63    | 45    | 42    | 25    | 62    | 45    | 76    | 63    |
| c'                | 12    | 9      | 14    | 12    | 12    | 9     | 14    | 12    | 16    | 14    |
| $\phi$            | 49    | 27     | 62    | 48    | 45    | 32    | 61    | 48    | 72    | 62    |
| Z                 | 4.5   | 4.5    | 4.5   | 4.5   | 2     | 2     | 5     | 5     | 7.5   | 7.5   |
| $\alpha$          | 38    | 38     | 38    | 38    | 42    | 42    | 42    | 42    | 42    | 42    |
| F                 | 2.06  | 0.97   | 3.28  | 2     | 1.93  | 1.26  | 2.9   | 1.83  | 4.75  | 2.94  |
| A <sub>crit</sub> | 0.653 | -0.018 | 1.404 | 0.616 | 0.622 | 0.174 | 1.271 | 0.555 | 2.509 | 1.298 |

|                   | 14    |       | 15    |       | 16    |       | 17   |       | 18    |       |
|-------------------|-------|-------|-------|-------|-------|-------|------|-------|-------|-------|
|                   | mean  | min   | mean  | Min   | mean  | min   | mean | min   | mean  | min   |
| RMR               | 72    | 65    | 55    | 37    | 56    | 36    | 57   | 37    | 74    | 47    |
| c'                | 15    | 14    | 13    | 11    | 13    | 11    | 13   | 11    | 16    | 12    |
| $\phi$            | 69    | 64    | 56    | 41    | 56    | 41    | 57   | 41    | 71    | 49    |
| Z                 | 7.5   | 7.5   | 3     | 3     | 10    | 10    | 2    | 2     | 3     | 3     |
| $\alpha$          | 42    | 42    | 45    | 45    | 45    | 45    | 45   | 45    | 45    | 45    |
| F                 | 4.04  | 3.2   | 2.41  | 1.49  | 2.19  | 1.31  | 2.64 | 1.62  | 4.49  | 1.91  |
| A <sub>crit</sub> | 2.034 | 1.472 | 0.997 | 0.346 | 0.841 | 0.219 | 1.16 | 0.438 | 2.468 | 0.643 |

|                   | 19    |       | 20    |       | 21   |       | 22    |       | 23    |       |
|-------------------|-------|-------|-------|-------|------|-------|-------|-------|-------|-------|
|                   | mean  | Min   | mean  | min   | mean | min   | mean  | min   | mean  | Min   |
| RMR               | 74    | 47    | 64    | 53    | 69   | 33    | 65    | 33    | 62    | 32    |
| c'                | 16    | 12    | 14    | 10    | 15   | 10    | 14    | 10    | 14    | 10    |
| $\phi$            | 71    | 49    | 63    | 38    | 67   | 38    | 64    | 38    | 61    | 37    |
| Z                 | 5     | 5     | 4     | 4     | 7.5  | 7.5   | 1     | 1     | 15    | 15    |
| $\alpha$          | 42    | 42    | 42    | 42    | 42   | 42    | 42    | 42    | 42    | 42    |
| F                 | 4.57  | 1.89  | 3.18  | 1.35  | 3.66 | 1.26  | 4.07  | 1.89  | 2.76  | 1.17  |
| A <sub>crit</sub> | 2.389 | 0.596 | 1.459 | 0.234 | 1.78 | 0.174 | 2.054 | 0.596 | 1.178 | 0.114 |

Table 1. Slope stability analyses calculated from in situ data and laboratory testing.



Figure 7. Clearance of rock slide debris from I8 near Techi

Therefore, while it is clear that extensive slope instability developed, it is unclear why this happened. A glance at the critical acceleration values shown in table 1 indicates that in many cases ground motions in excess of 1 g were required to induce movement of the slope. This is clearly at odds with the reported ground motions caused by this event. Even *nearfield* ground accelerations were found to be in the order of 0.98 g, and the epicentre of the earthquake was some distance (approximately 60-70 km) from the site of these landslides. It can be seen that the ground motions required *merely to initiate movement*, not induce

complete slope failure, were somewhere of the order of 200-300% greater than the peak motions recorded during this event. Therefore, it is necessary to ask whether slope failure occurred due to unforeseen rock mass qualities, or through unexpectedly high ground motions (or indeed, some combination of the two).

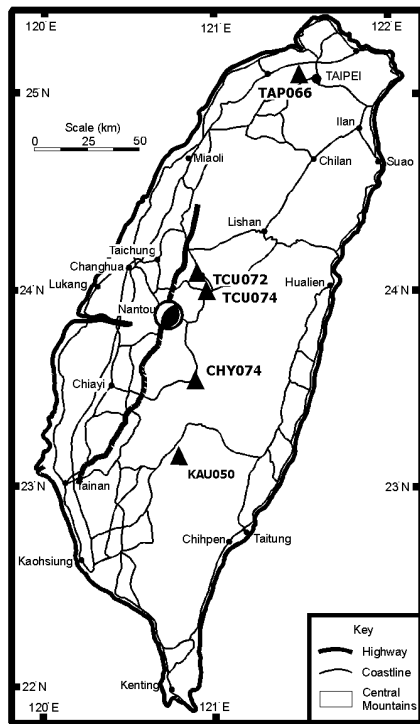
### 3.4 Ground motion data

Analysis of ground motions remains at this point somewhat preliminary. However, a selection of accelerometer data collected by the Chinese Weather Bureau (CWB) from the network of stations in Taiwan has been corrected, and response spectra have been calculated from these records. Figure 8 and figure 9 show the locations and the spectra of 5 accelerometer stations located in nearfield and farfield locations. These diagrams show curves at 20%, 10%, 5% and 2% of critical damping. Also shown on these diagrams is the peak recorded ground motions and the epicentral distance. On the basis of even a cursory study of these data, it is possible to make some general observations:

1. the amplitude of earthquake ground motions decreases with distance from the epicentre;
2. the high frequency component observed in stations TCU072 and TCU074 are strongly attenuated with distance;
3. significant high frequency components of the spectrum can still be observed in the farfield.

While these observations may not be unusual; similar observations have been reported in several earthquakes, it is useful to consider some of these data in light of the unexpectedly high incidence of slope failure at near the Techi Dam.

The data from the two nearfield stations (TCU72 and TCU74) show spectra which are dominated by frequency modes at about 0.5s (2Hz) and 0.75 s (1.3 Hz) in the East-West direction. Both stations show long tails of high frequency data in the range of 0.2 – 0.05 s (5-20 Hz). The spectral accelerations of these motions is approximately  $5\text{ms}^{-2}$  (approximately 0.5 g). The ground motion data in the North-South orientation show similar characteristics, although the spectral



Response spectra for three 'nearfield' stations showing decreasing vertical ground motion with distance (data courtesy of Chinese Weather Bureau, Taipei)

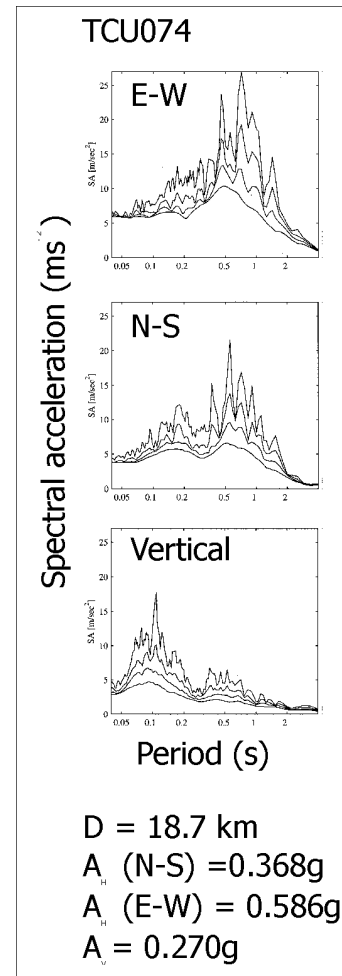
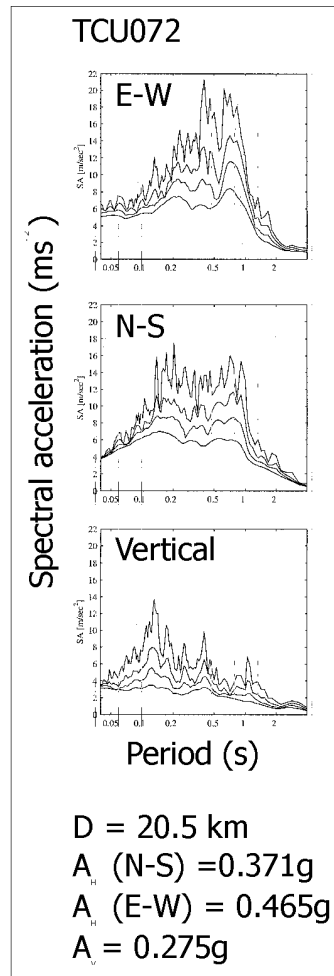


Figure 9. Response spectra calculated from accelerometer data collected from stations TCU072 and TCU074

accelerations of these motions is somewhat higher in the East-West direction: 20-26  $\text{ms}^{-2}$  (2-2.6g) in the East-West direction as opposed to 18-20  $\text{ms}^{-2}$  (1.8-2.0g) in the North-South mode at 2% damping. Additionally, in the case of both nearfield stations, high vertical ground motions can be observed, the peak spectral acceleration values fall in the range of 14-18  $\text{ms}^{-2}$  (1.4 – 1.8 g) with the peak values being mobilised at the high end of the spectrum. These values decrease of course with increasing damping.

The farfield stations show somewhat differing responses. Notably, the high frequency content of the ground motions recorded at KAU050 which although showing considerably lower values of spectral acceleration (2-2.5  $\text{ms}^{-2}$  horizontal and 0.5-1  $\text{ms}^{-2}$  vertical ground motions) shows a ground motion profile which is dominated by higher frequencies. Similarly, for station CHY074 there is a component of high frequency shaking observed in the horizontal and vertical response spectra. The station with the largest distance between the earthquake epicentre and the recording instrument (TAP066) shows a shift towards the maximum response being mobilised at higher natural periods (i.e. lower frequencies.)

#### 4. DISCUSSION

On the basis of preliminary results on selected stations it is difficult to draw firm comparisons. It is however possible to make some useful observations at this point. Stations TCU072 and

TCU074 are close to the epicentre, and, it would be expected to be dominated by high frequency ground accelerations. The stations which are most interesting from the point of view of the landslides near at the Techi Dam are stations CHY074 and KAU050. These bracket the distance between the epicentre and the failures on the Central Cross Island Highway. Furthermore, these stations are found at high elevations, with KAU050 at 640 m and CHY074 at 2413 m above sea level. Therefore, these two stations are most likely to give a reasonable indication of the ground motions experienced at the site of the landslide activity.

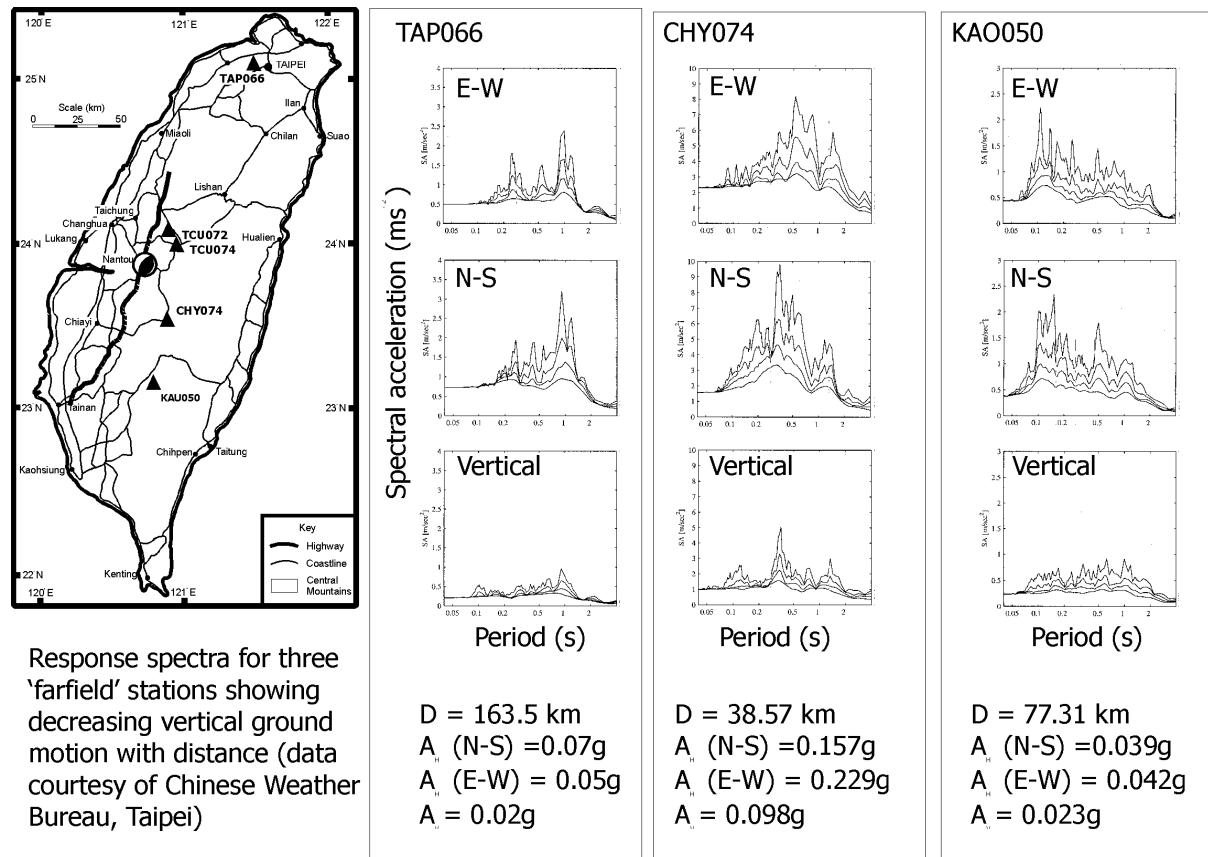


Figure 10. Response spectra calculated from strong motion data collected at stations TAP066, CHY074 and KAU050

It has been noted that the resonant frequency of hard rock masses tends to lie at the upper end of the frequency spectrum (Seed and Idriss, 1982). Normally, strong rock masses will resonate at a range of values between 8 and 20 Hz. Therefore, it is tempting to assume that failures near the Techi Dam site were the result of the resonance of the rock mass giving rise to unusually high ground accelerations. Indeed the range of frequency values observed in stations CHY074 and KAU050 do tend to support this interpretation.

In addition to simple resonance there are likely to have been topographic effects related to the slope height and angle. It is notable that there is a large increase in the incidence of landslides triggered by the earthquake in this terrain. It has long been recognised that canyons show unusual levels of ground motion during strong earthquakes. However, it is worth remembering that while this rock mass is dominated by strong sandstone units, there is also a significant proportion of weak shales and slates, as well as large discontinuities. All of these factors will affect the shear wave velocity of the rock mass.

Both nearfield and farfield ground motions show differences between the N-S and E-W oriented accelerometer data relating to horizontal ground motions. It is also noticeable that the major discontinuities observed in the rock mass i.e. the bedding dips in an easterly manner. However, this is a regional dip, and if it is necessary to seek an explanation of unexpectedly high ground motions on the basis of changes in ground motion direction, then it remains difficult to explain why there was such a marked difference in slope response to shaking further east of the Techí Dam. The marked difference in landslide incidence between the east and west of Techí cannot be explained by simple attenuation, nor can it be explained by differences in the stability of the slopes under normal conditions. Geomorphological evidence would tend to suggest that the weaker rock masses to the east of the Techí Dam are in fact *more* susceptible to landsliding, and if both rock masses were responding to similar forces, there should be a higher incidence of slope failure to the east of Techí, rather than the west.

Additionally, the actual slope stability analysis model makes assumptions about the behaviour of the rock mass, some of which may be invalid. The infinite slope model is highly sensitive to the cohesion term in the strength component of the rock or soil mass, and therefore slopes with a high cohesive, or apparent cohesive, strength may in fact over-estimate the stability of the slope. The way in which rock masses are likely to respond to earthquake shaking is likely to be complex: with no tensile strength along fractures, the rock mass is likely to respond to different shaking directions in an unusual manner.

This observation tends to support the view that some interaction between the ground motions, and the canyon topography west of the Techí Dam. It seems likely that high frequency ground motions have interacted with the competent rock mass in order to cause large scale slope failure. On the basis of the response spectra considered to date, it is difficult to say whether horizontal or vertical ground motions were responsible, but clearly there has been slope behaviour which is currently unpredicted by existing models of ground motions during earthquakes.

It is notable that the Spectral acceleration values ( $S_a$ ) are much more similar to the value of  $A_{crit}$  required to induce slope movement. It seems likely therefore, that as in the calculation of base shear coefficients for buildings, slope stability analysis under earthquake loads should be carried out on the basis of calculated response spectra, at frequencies appropriate to the ground conditions.

## **5. CONCLUSIONS**

It is difficult to draw too many conclusions on what has been largely descriptive form of investigation. However, there are a few comments which can usefully be made:

1. landslides triggered by the Chi Chi earthquake near Techí occurred in rock masses which show high factors of safety under static conditions;
2. these landslides were largely associated with the presence of weak mudstone layers within the stratigraphy. Even assuming the worst case rock mass criteria the slopes, with one exception, still show high factors of safety.
3. there was a marked increase in the incidence of landslides between east and west of the Techí Dam. This may be explained by changes in geology. This said, it still seems likely that resonant frequencies of the rock masses remain higher than 8 Hz.

4. The markedly high incidence of landslide activity west of the Teché Dam occurred in an area of steep canyon topography. It seems likely that there has been an interaction between the geology, topography and the incident seismic waves to generate ground motions 2-3 times higher than suggested by accelerometer data from the area.
5. It may be necessary to revise current methods of slope stability analysis during earthquakes in terms of the inputs used, as there appears to be serious limitations in the use of peak horizontal ground acceleration, and current 'pseudo-static' slope stability models.

Future research which will seek to support field observations with more detailed analysis of the rock mass properties and the static stability of slopes. Additionally, further processing of the data acquired from the CWB as well as information from the Bureau of Dams will hopefully yield further information about the character of ground motions experienced in this area during the earthquake.

## 6. ACKNOWLEDGEMENTS

The authors wish to acknowledge the financial support of the Natural Environment Research Council (research grant number:GR3/12975) which enabled fieldwork to be carried out after the earthquake. Dr Patrick Smit of the Engineering Seismology and Earthquake Engineering Division is thanked for processing and correcting strong motion data that the Chinese Weather Bureau kindly provided.

## 7. REFERENCES

- Bieniawski, Z. T. 1989. *Engineering Rock Mass Classification*. Wiley, New York.
- Bilham, R. & Yu, T. T. 2000. The morphology of thrust faulting in the 21 of September 1999, Chi Chi, Taiwan earthquake. *Journal of Asian Earth Sciences*, **18**, 351-367.
- EPOCH (European Community Programme) 1993. *Temporal Occurrence and forecasting of landslides in the European Community*. Flageollet, J. C. (Ed), 3 volumes, Contract No. 90 0025.
- Hoek, E. 1994. The strength of rock and rock masses. *News Journal*, International Society of Rock Mechanics, **2**, 4-16.
- Newmark, N. M. 1965. Effects of earthquakes on dams and embankments. *Geotechnique*, **15** (2), 139-160.
- Jibson, R. W. 1987. Summary of the research on the effects of topographic amplification of earthquake shaking on slope stability. *Open-file report 87-268*, United States Geological Survey, Menlo Park, California.
- Jibson, R. W. & Keefer, D. K. 1993. Analysis of the seismic origin of landslides: examples from the New Madrid seismic zone. *Bulletin of the Seismological Society of America*, **105**, 521-536.
- Onodera, T. F. 1963. Dynamic Investigation of Foundation Rocks. *Proceedings of the 5<sup>th</sup> Symposium on Rock Mechanics*, Minnesota, 517-533, Pergamon Press, New York.
- Seed, H. B. & Idriss, I. M. 1982. *Ground motions and soil liquefaction during earthquakes*.

Earthquake Engineering Research Institute, Berkeley, California, 134pp.

Shieh, C. I. 1991. A case history of slope stabilisation at the Techii Reservoir, Taiwan. *In* Cosgrove, J & Jones, M. E. (Eds), *Neotectonics and Resources*, 326- 341.

Shin, , T. C., Kuo, K. W., Lee, W. H. K., Teng, T. L. & Tsai, Y. B. 2000. A preliminary report on the 1999 Chi Chi (Taiwan) earthquake. *Seismological Research Letters*, **71** (2).

Varnes .D. J. 1978. Slope movement types and processes. In: R. L. Schuster and R. J. Krizek (eds), Special Report 176: *Landslides: Analysis and Control*, Washington, TRB, National Research